THE INTERNATIONAL JOURNAL OF SCIENCE & TECHNOLEDGE

Adsorption of Cu and Pb by ZnO Nano Rods Prepared by Microwave Hydrothermal Method

A. M. Abdelhady
Ph.D. Student & Assistant Lecturer, Central Laboratory for Elemental & Isotopic Analysis, Nuclear Research Centre, Atomic Energy Authority, Cairo, Egypt
S. A. Abd El Aal
Lecturer, Central Laboratory for Elemental & Isotopic Analysis, Nuclear Research Centre, Atomic Energy Authority, Cairo, Egypt
M. M. El-Okr
Professor, Physics Department, Faculty of Science, Al-Azhar University, Cairo, Egypt
A. I. Helal
Professor, Central Laboratory for Elemental & Isotopic Analysis, Nuclear Research Centre, Atomic Energy Authority, Cairo, Egypt

Abstract:
In the present work, ZnO nano-rods are prepared by microwave assisted hydrothermal method at different pH values. Crystal structure and phase purity of prepared ZnO Nano-rods were investigated by x-ray diffraction. Impurities free powder is studied by x-ray florescence spectrometer. The morphology of prepared ZnO nano-rods is assured by means of field emission scanning electron microscope. Batch experiments are performed for the removal of lead and copper ions, from their aqueous solutions, by using ZnO nano-rods as adsorbents. Adsorption parameters such as solution pH, adsorbent dosage and contact time are studied by using ICP-OES to reach the optimum conditions for removal of Pb and Cu from aqueous medium. Sorption equilibrium isotherm is described by fitting experimental data obtained with both Freundlich and Langmuir models. Furthermore, for kinetic studies, pseudo-first order and pseudo-second order models are applied and compared with experimental dat.

Keywords: *Microwave hydrothermal, chemical co-precipitation, Nano-rods, adsorption, and heavy metals adsorption*

1. Introduction

Recent progress in industrial activities had lead to heavy element contamination of groundwater and surface due to industrial waste. Heavy elements have hazardous effects on ecosystem, especially on human being when they are at levels more than threshold limits [1]. For these reasons, the need for processes to remove heavy elements has received increasing attention [2-4]. There are several methods commonly used for removal of heavy metals from aqueous solution include ion-exchange [5], chemical precipitation [6], nano-filtration [7], solvent extraction [8], reverse osmosis [9] and adsorption methods [10]. Under certain conditions, some of these methods are more effective. However, adsorption offers flexibility in design, operation, and in many cases, it generates high quality treated effluent. In addition, in many cases the adsorbents can be regenerated by suitable desorption processes for multiple use. In addition, many desorption processes are highly efficient, lowly costive maintenance, and easily of operation [11]. It is also applicable to implement adsorption in full-scale and the process methods are time consuming. Therefore, the adsorption process is considered one of the most major techniques for heavy element removal from water/waste water [12].

According to the points mentioned above, researchers do great efforts to construct and design new, low cost and non-toxic adsorbents able to remove heavy element pollutants and eliminate their levels to values lower than maximum allowable content [13].

Thus, several organic and inorganic adsorbents have been synthesized for the use in heavy elements removal, including clay minerals, bio-sorbents, zeolites, fly ash, and activated carbon [14-19]. In the last few decades, there were large amount of interest in the use of Nano-materials for removing heavy metals from different types of matrices [20]. Nano-materials have several unique properties; of these properties as benefits in heavy elements removal. Nano materials usually have high surface area, high adsorption capacity, unsaturated surfaces, simple operation, and simple production [21]. Nano-materials such as nano zero-valent iron (NZV Fe), Fe_2O_3, Fe_3O_4, TiO_2, SiO_2, and Al_2O_3 are the most commonly used materials that have been applied as adsorbents [22].

Nano-sized metal oxides are highly active for a large numbers of reactions that are important in both chemical synthesis and pollution control [23]. Zinc oxide (ZnO) is one of the most important multifunctional oxide materials that used in industrial applications. Zinc oxide (ZnO) is an n-type semiconductor with a wideband gap of 3.37 eV. It has been widely used in many industrial applications such as ceramics, chemical sensors, piezoelectric transducers, photo-catalysts, anti-UV additives, microwave absorbers and etc. [24]. ZnO is an environmental friendly material. It can be used in gas sensors, industry as a catalyst, electrical and optical devices, solar cells-chemical absorbent and etc. [25-27].

ZnO was mostly applied to eliminate H_2S but now researchers have found that nano-structured ZnO could efficiently remove heavy metals [28]. There are several physical and chemical techniques for preparing ZnO nano-particles. For instance, a variety of methods can be used to control ZnO particle size, aspect ratio, surface area and shape in the nanometer range [29-31]. Different synthesis methods have been devised, including micro-emulsion, sol–gel synthesis, vapour transport process, mechano-chemical processing, sono-chemical or microwave-assisted hydrothermal synthesis [25-28].

Microwave assisted hydrothermal processing of nano-materials is fundamentally different from the conventional heat processing in terms of the heat generation mechanism. In a microwave processing, heat is generated within the media of the sample itself by the interaction of microwaves with the material. Conventional heating generates heat by heating container walls; then the heat is transferred to the surface of sample [32]. Microwave processing of materials have some important benefits, since it produces uniform and volumetric heating (due to deep energy penetration), improved quality and properties, short processing times and synthesis of new materials, where processing not possible with conventional means [32].

In the present work, ZnO nano-rods like structure is prepared by microwave assisted hydrothermal method at different pH values. Crystal structure and phase purity of prepared ZnO nano-rods is tested by x-ray diffraction (XRD). Impurities are investigated by x-ray florescence spectrometer (XRF). The morphology of prepared ZnO nano-rods is observed by means of scanning electron microscope (SEM). Batch experiments are performed for the removal of lead and copper ions, from their aqueous solutions, by using ZnO nano-rods as adsorbents. Adsorption parameters, such as solution pH, adsorbent dosage and contact time, are studied to reach the optimum conditions for removal of Pb and Cu from aqueous medium.

2. Experimental

2.1. Materials and Methods

Chemical materials used for preparing ZnO nano particles are zinc chloride ($ZnCl_2$) as the zinc cation precursor and sodium hydroxide (NaOH) as the hydroxide anion precursor. De-ionized (DI) water (18MΩ) was used in all preparation procedures. Stock solution of 1000 ppm single element standard of Pb and Cu was used in adsorption experiments. All Chemicals and reagents are of analytical grade and used without further purification.

2.2. Preparation of ZnO nano Particles

ZnO nanostructure was prepared by co-precipitation microwave-assisted hydrothermal method [32]. For this purpose, the concentration ratio between zinc chloride and sodium hydroxide was 1:2, respectively. Hence, 0.3M of $ZnCl_2$ was prepared by dissolving 4g of $ZnCl_2$ in 29 mL of DI water and 0.6M of NaOH was prepared in 20 mL of DI water separately. Then, zinc chloride solution and NaOH solution were mixed slowly by placing the beaker containing $ZnCl_2$ solution on a stirring hot plate, then NaOH solution was slowly added into it using a syringe under vigorous stirring. During the addition of NaOH, formation of white precipitates of zinc hydroxide was observed. Starting pH was 2.7, and the temperature slightly increased to about 35–45 ˚C during the precipitation process. The precipitation was carried out until the desired temperature compensated pH of about 5-9 was achieved. The total precipitation time was about 30 min. The slurry was subsequently agitated for another 10 min in order to stabilize the pH value. The slurry was then transferred to 100mL Teflon container. The container was closed with screw cap, placed in a special Teflon holder and then transferred to a microwave oven (ETHOS, 2.45 GHz, maximum output power 1200 W, USA). After completing the interaction, the containers were kept 10 min in ventilation mode and then kept for cooling in room temperature. Samples were filtered using 0.45µm whattman filter paper and then washed several times with DI water. After using at least 300 mL of DI water for washing, all water was filtered off and the remaining powder was placed on a vacuum drying system for 10 h, the dried powder was collected and prepared for analysis. To study the crystal structure and phases of prepared ZnO, XRD (Shimadzu6000, Japan) was used. The used X-Ray tube is a copper-tube operating at 40 kV and 30 mA and the used wavelength is $K_{\alpha 1}$ with wavelength 1.54056 Å. The scan was performed over the range 2Θ (10-90) degrees. The identification of the present crystalline phases was done using Joint Committee on Powder Diffraction standards (JCPDS) database card numbers. XRF (JSX-3222 analyzer, Joel, Japan) was used for measuring the purity of product samples. For morphology and structure studies, the samples were inspected by field emission scanning electron microscope using a FEI instrument (Quanta FEG 250 model in NL, USA).

2.3. Batch Adsorption Experiments

Batch adsorption experiments were carried out to study the ability of ZnO to work as an adsorbent for removing Pb and Cu ions from their aqueous solution. For this purpose, experiments were conducted in a series of 50 mL Falcon tubes containing 0.05 g (2 g L^{-1}) of nano structured ZnO powder with 25 mL of 100 mg L^{-1} metal ions solution. The suspensions were shacked on a mechanical shaker at 300 rpm and room temperature (25^{o}C). Solid/liquid phases were then separated by filtration through a 0.45 µm whattman filter paper. The supernatants were then taken and the concentration of heavy elements was measured by inductively coupled plasma optical emission spectrometer (Leeman Prodigy Prism High Dispersion ICP-OES, USA). The percentage of removal (R) was calculated as:

$$\%\text{Removal} = ((C_0 - C_e)/ C_0) \times 100$$

Where, C_0 and C_e are initial and final concentration of heavy element in the solution phase.

To study the effect of pH on removal ratio of Pb and Cu ions, batch experimental procedures were conducted at different pH values. pH value was adjusted by adding HCl or NaOH to obtain the analyte solution pH range from 5 to 9, then the solutions were shacked at 300 rpm for 20 min at room temperature. For studying the effect of contact time, batch experimental procedures were conducted with different shaking times of: 10, 30, 50, 60, 90, 120, and 180 min, while other conditions were remained constant at 7 pH value and room temperature. The effect of ZnO nanoparticles dosage on the removal of Pb and Cu ions was studied by shaking 25 ml of 100mg/l Pb and Cu single solution using different weights of ZnO nano particles(0.01, 0.02, 0.05, 0.1 and 0.15 g) and shacking the solutions at 300rpm for 20 min at 7 pH value and room temperature.

3. Results and Discussion

3.1. Characterization of Prepared ZnO

3.1.1. XRD and XRF Analysis

Phase purity and crystal structure of prepared ZnO were investigated using XRD. Fig1 shows XRD pattern for prepared ZnO by microwave assisted hydrothermal method at different pH values (5,7 and 9values). Samples were prepared at 500W RF power, 100 ^oC and 10 minutes interaction temperature and time respectively. All diffraction peaks are indexed to the hexagonal phase of ZnO (JCPDS 36-1451) and no other crystalline phases are detected. All diffractograms show the nine prominent peaks of ZnO. The characteristic peaks with high intensities correspond to the (100), (002), (101) planes and lower intensities are corresponding to the (102), (110), (103), (200), (112), (201) planes, indicates that the products are of high-purity hexagonal wurtzite structure (the most stable phase of ZnO) [34]. Since all peaks are highly intense and narrowed, this reveals that the formed products have a good crystallinity. XRD analysis has revealed high level of crystallinity and 100% phase purity of ZnO powders prepared. Only XRD peaks derived from the ZnO (zincite) phase were observed in all cases. Purity of prepared ZnO powder was tested by XRF analysis Figure 2. The mean grain size (D) of prepared ZnO was calculated by using Scherrer equation to the (101) plane diffraction peak (2θ=36.2°). The crystalline grain sizes of ZnO samples, which were prepared by microwave irradiation method at different pH values, are presented in Table1 where the grain size was varied from 25-47 nm.

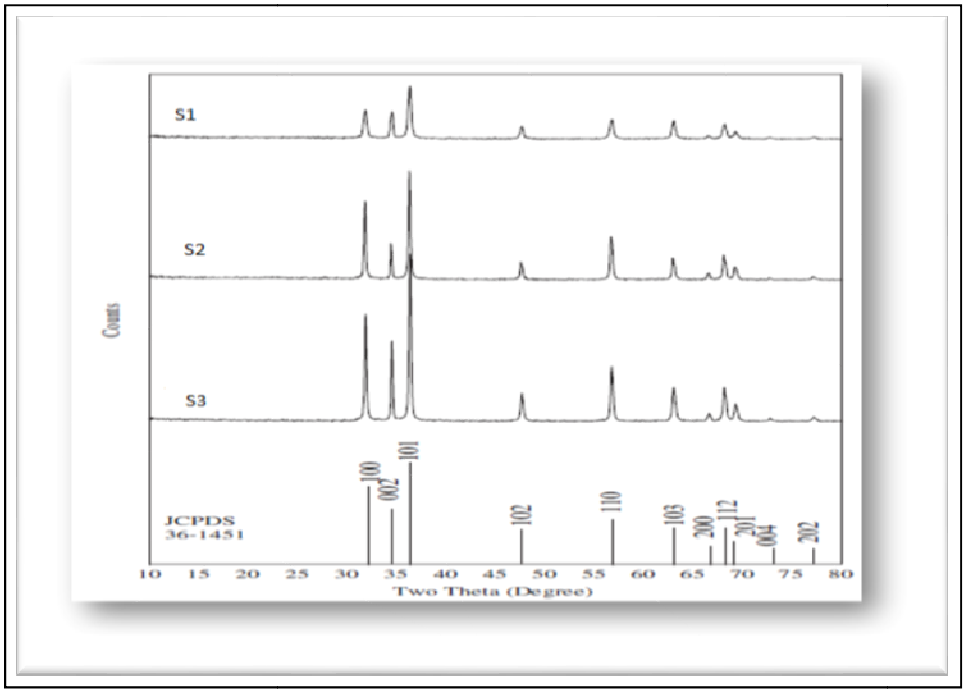

Figure 1: XRD for prepared ZnO nano rods at different pH 5(S1), 7(S2) and 9(S3)

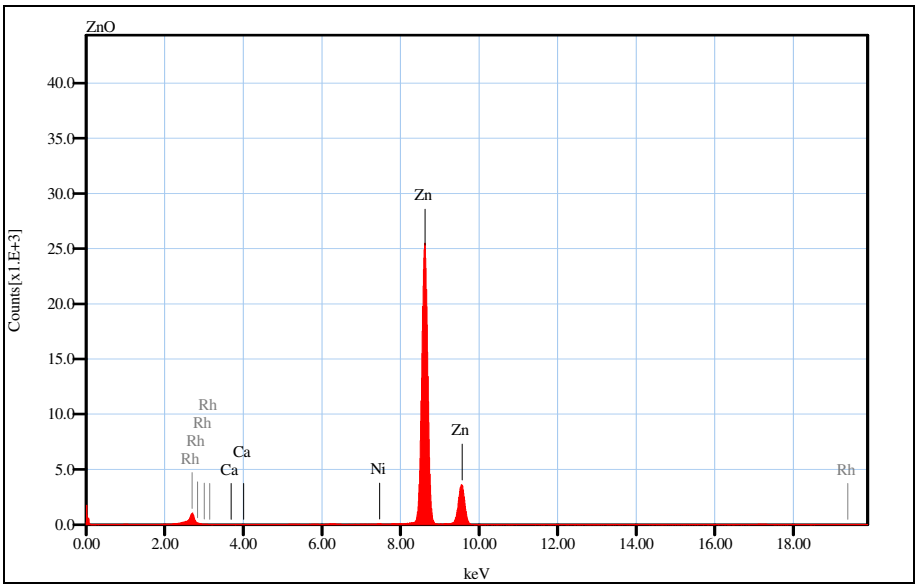

Figure 2: XRF shows chemical composition of prepared ZnO nano-rods

Sample	pH	D (nm)	Lattice parameters		
			a (A^o)	c (A^o)	c/a
S1	5	47.33	3.243	5.2	1.6
S2	7	43.1	3.25	5.21	1.6
S3	9	25.6	3.247	5.2	1.6

Table 1: Data calculated from XRD

3.1.2. ZnO Morphology and SEM Analysis

The surface morphology of prepared ZnO, at different pH values, was analyzed using scanning electron microscope (SEM) as shown in Figure 3. In agreement with previous work [35], all SEM micrographs reveal that, the different pH of the precursor solution affect particle size, diameter and length of nano rods but not their morphology. Figure 3 shows the SEM images of zinc oxide nanorods obtained at different values of pH. For all samples, nanorods were obtained but with varying aspect ratios. When pH value was 5 (Figure 3a), the nanorods were shorter and smaller than those obtained at pH 7 and 9 (Figure 3b and Figure 3c, respectively). The enhanced growth in alkaline solution has been reported where the abundance of OH^- contributed to the formation of the intermediate molecule, $Zn(OH)_2$ which facilitated the formation of ZnO [36]. However, these results showed that, there seemed to be little difference between ZnO nanorods synthesized using neutral (Figure 3b) and alkaline (Figure 3c) solutions. The shorter and smaller diameter nano-rods obtained using acidic solution can be attributed to the preferential erosion of the (0001) compared to other ZnO crystal faces [36]. From the SEM images the aspect ratio of ZnO nano-rods synthesized in acidic solution were about 5 and those synthesized in alkaline and neutral solution were about 10.

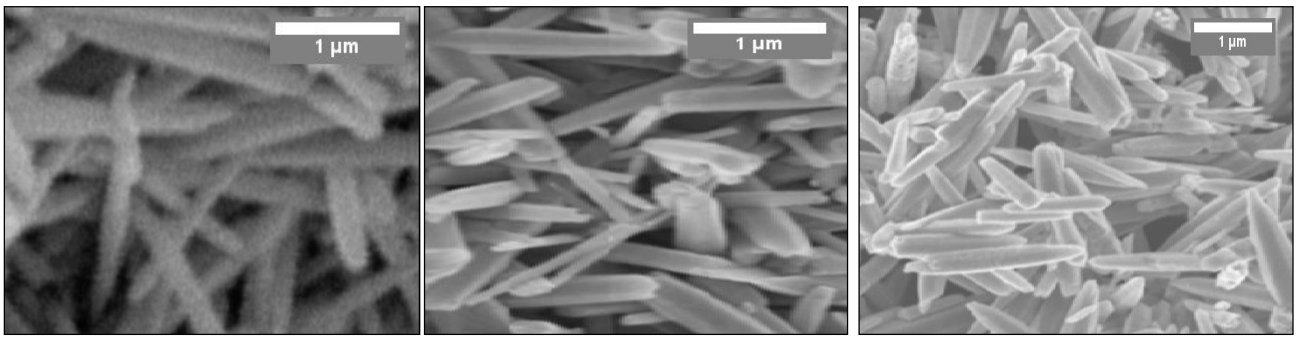

(a) *(b)* *(c)*

Figure 3: SEM image of ZnO NPs prepared at different pH values a) pH5, b) pH7 and c) pH9.

3.2. Sorption Investigations

3.2.1. Effect of pH

Surface charge of the adsorbent is influenced with Hydrogen ion concentration (pH of the solution), the degree of ionization and the species of adsorbate. Therefore, the initial pH value of the solution is an important parameter in the adsorption process of metal ions

from aqueous solutions, which affect both the dissociation degree of functional groups from adsorbent surface and the speciation and solubility of metal ions [37].

The effect of pH of solution on the adsorption of $Pb^{+2}$and Cu^{+2}ions by ZnO, as adsorbent, was investigated by changing pH of solution from 2 to 9 and keeping other parameters constant. The highest removal percentage occurred at pH 7 for both lead and copper ions in the order: ***Cu (97%) >Pb (92.3%)*** as shown in Figure 4**.** It can be observed from the inspection of Figure 4 that, the adsorption of $Pb^{+2}$and Cu^{+2}ions on ZnO NPs is very sensitive to pH value of the solution. The low adsorption at low pH, may be related to the fact that, the higher concentration and higher mobility of H^+ ions present in solution favored the preferential adsorption of hydrogen ions compared to $Pb^{+2}Cu^{+2}$ions.

It would be possible to suggest that at lower pH value, the surface of the adsorbent is surrounded by hydronium ions (H_3O^+), which prevent the metal ions from approaching the binding sites of the sorbent [38]**.**

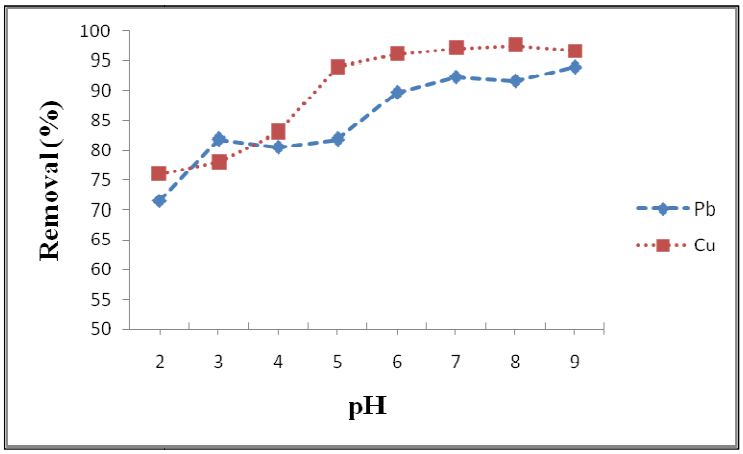

Figure 4: Effect of pH on the removal of Pb and Cu ions using ZnONPs:(V = 25 ml, time=50 min, C_o=70 mg/L, adsorbent dose=0.05 g and shaking speed=300 rpm)

Thus, the highest removal efficiency for lead and copper with ZnO adsorbent was obtained at pH=7.0 due to the excess amount of OH^- ions within the medium and the active site on adsorbent materials which are negatively charged. This causes a strong attraction between these sites and the positively charged metal ions. Therefore, the optimum pH value of aqueous solution for adsorption is considered to be 7. At this optimum pH, the limited adsorption sites will be fully occupied and no further increase in Pb and Cu ions adsorption was observed at higher pH values [38]**.**

3.2.2. Effect of Adsorbent Dosage

The effect of ZnO NPs, as adsorbent, doses on removal efficiency of Pb and Cu ions was investigated by varying adsorbent weight from 0.01 to 0.1 g/25mL (0.4to 4 g/L) and keeping other parameters constant (V = 25 ml, time=50 min, C_o=70 mg/L, pH=7.0 and shaking speed=300 rpm). Figure 5 shows the Effect of adsorbent dose on removal efficiency of Pb and Cu ions using ZnO NPs. In this concern, the removal percentage of $Pb^{+2}$and $Cu^{+2}$was increased by increasing adsorbent dose as mentioned previously. This result is expected, since as the weight of adsorbent increases, the number of active sites of adsorbent increases [39]**.** Figure 5 shows that there was no significant change on adsorption efficiency by increasing adsorbent dose more than 0.075g. Thus, the optimum adsorbent dose that can be considered is 0.075 g/25mL (3 g/L). The order of removal percent under these conditions is: ***Cu (93.9%)>Pb (91.7%)***.

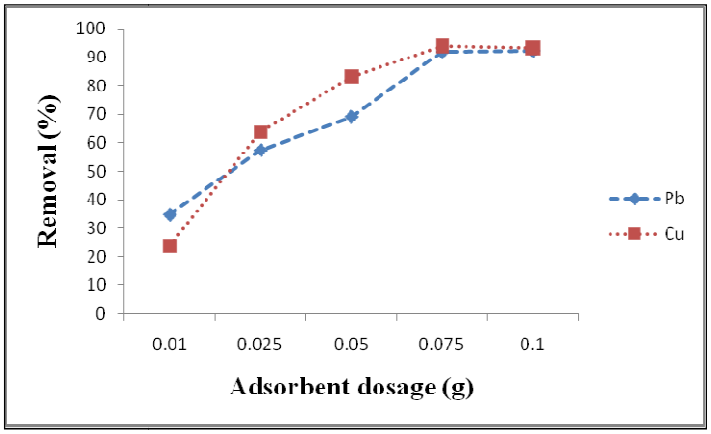

Figure 5: Effect of adsorbent dose on the removal of Pb and Cu ions using ZnOas adsorbent. (V = 25 ml, time=50 min, C_o=70 mg/L, pH=7.0and shaking speed=300 rpm)

3.2.3. Effect of Contact Time

The effect of contact time on the adsorption of Pb and Cu ions by ZnO NPs, as adsorbent, was investigated by varying the shaking time between the adsorbate and adsorbent in the range 10 - 300 minutes. Figure 6 shows the relation between removal percentage of Pb and Cu ions and the contact time. The initial concentration of Pb and Cu was 100 mg/L, while the dosage of nano adsorbents was 0.05 g/25 ml (2 g/L). Figure 6 shows that the removal efficiency of Pb and Cu ions has reached maximum values after100–150 min. After more than 150 minutes, no significant increase in the removal percentage can be occurred, which may indicate that, adsorption has already achieved equilibrium. Maximum adsorption of metal ions has been reached and no further removal occurs even for longer shaking time. Thus the optimum shaking time was determined as 100 minutes. The order of removal (%) on ZnO NPs as sorbents is: ***Pb (92%)=Cu (92%).***

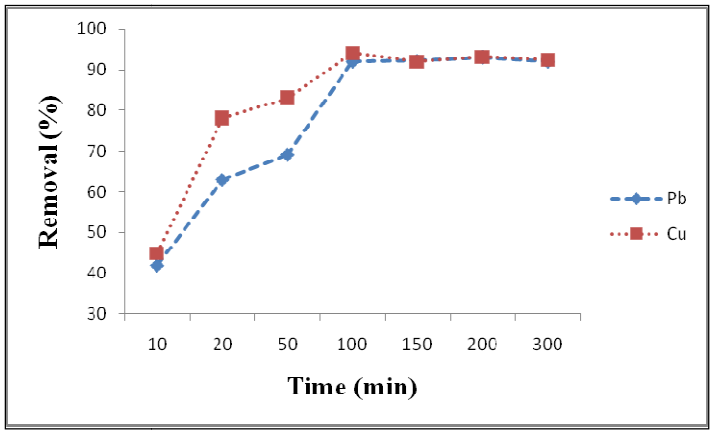

Figure 6: Effect of contact time on the removal of Pb and Cu ions using nano ZnO. (V=25 ml, W=0.05 g, Co=100 mg/L, pH=7.0 and shaking speed=300 rpm)

3.2.4. Adsorption Isotherms

Adsorption isotherm is required for the design and dimensioning of the adsorption process. Langmuir and Freundlich models are most frequently used for describing equilibrium adsorption isotherms [40]. In order to evaluate whether the adsorption processes is applicable or not, the initial concentrations of Pb and Cu ions in the range of 20–200 ppm have been prepared for the investigation of the adsorption isotherm. The adsorption isotherms of Pb and Cu ions from aqueous solution on to ZnO nano particles at room temperature are shown in Figure 7. In the present work, two models, both Langmuir and Freundlich, are used to analyze the data. The Langmuir equation, which is applied for monolayer adsorption onto a surface with a finite number of identical sites, can be expressed by:

$$\frac{C_e}{q_e} = \frac{1}{K_L q_m} + \frac{C_e}{q_m}$$

Where K_L is a constant of adsorption equilibrium (L mg^{-1}), and q_m is the saturated monolayer adsorption capacity (mg g^{-1}). A plot of C_e/q_e versus C_e yields a straight line with slope $1/q_m$ and intercepts $1/(q_m K_L)$. Another widely used empirical equation, the Freundlich equation, was based on adsorption on a heterogeneous surface. The equation is represented by:

$$q_e = K_f C_e^{1/n}$$

This equation can also be transformed into another linear form:

$$\log q_e = \log K_f + \frac{1}{n} \log C_e$$

Where q_e is the equilibrium metal uptake capacity; Ce denotes the residual metal concentration at equilibrium; and K_f and n are the Freundlich constants related to the adsorption capacity and adsorption intensity of the sorbent respectively. The essential features of the Langmuir isotherm may be expressed in terms of equilibrium parameter R_L, which is a dimensionless constant referred to as separation factor or equilibrium parameter which used for predicting the affinity of the ZnO nano rods to sorbate [41]. R_L is given by the relation:

$$R_L = 1/(1 + K_L C_o)$$

Where, R_L is equilibrium parameter, C_o is the initial concentration, and K_L is the constant related to the energy of adsorption (Langmuir Constant).

R_L value indicates the adsorption nature to be either unfavorable if $R_L>1$, linear if $R_L=1$, favorable if $0< R_L<1$ or irreversible if $R_L=0$ [41].

In this respect, the values of q_m and K_L are calculated from the slope and intercept of the Langmuir plot of C_e/q_e versus C_e. On the other hand, the values of K_F and n are calculated from the slope and intercept of the Freundlich plot of Log q_e versus Log C_e.

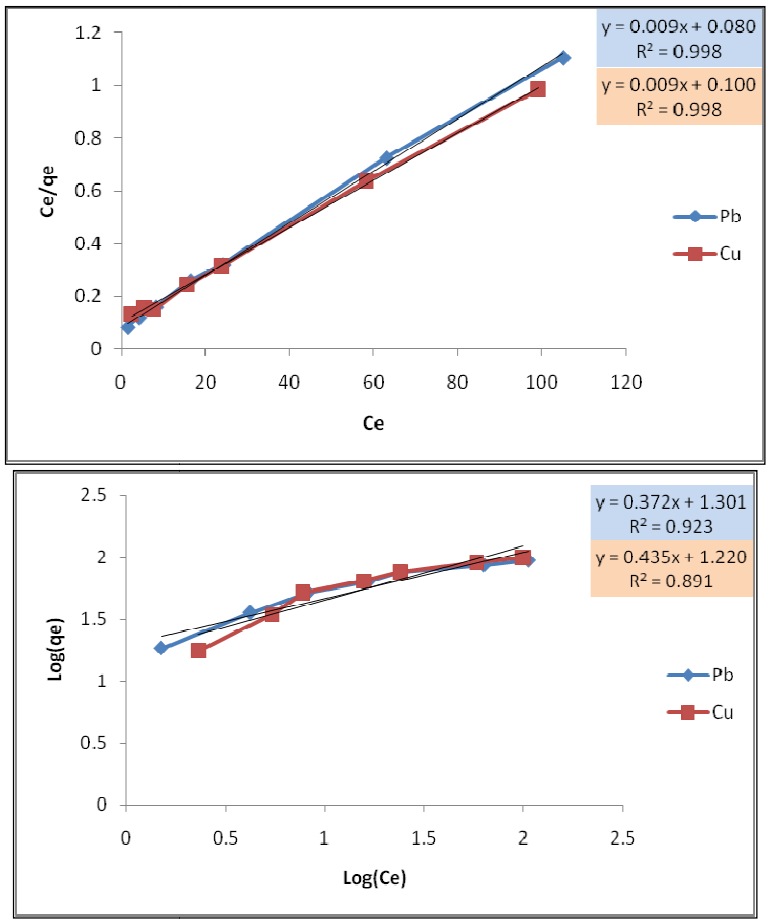

Figure 7: Linearized parameters of adsorption isotherm models for Pb(II) and Cu(II) on ZnO nanoparticles. a) Langmuir isotherm model and b) Freundlich isotherm model

Figure 7 shows the experimental data of Pb and Cu analyzed according to the linear form of the Langmuir and Freundlich isotherms. The adsorption pattern of Pb^{+2} and Cu^{+2} on ZnO nano particles were found to fit well with the Langmuir model with R^2 values of 0.998 for both lead and copper ions, which are higher than the case of Freundlich model (0.923 and 0.891 for Pb and Cu ions respectively). It is observed that, calculated q_m is 111mg/g for both Pb and Cu which is very close to experimental value (95 and 101 mg/g for Pb and Cu respectively). This sequence matches very well with the sequence that was obtained in case of batch experiments. Adsorption constants for both Langmuir and Freundlich are summarized in Table2. R_L values of adsorption of Pb^{2+} and Cu^{2+}on ZnO nano particles are 0.0011 and 0.0009 respectively (Table2). Since R_L values lie between 0 and 1, it is seen that the adsorption of heavy element ion is favorable [42].

K_F and n of Freundlich isotherm model are constants incorporating all factors affecting the adsorption capacity and intensity of adsorption, respectively. The values of K_F and n show the increase of negative charge on the surface which enhances the electrostatic force between the ZnO nano particles and both lead and copper ions, which increases in turn the adsorption of Pb^{2+} Cu^{2+}, the value of n is greater than one indicating that the adsorption is favorable [43].

Analyte Element	q_{max}, exp. (mg/g)	Langmuir model				Freundlich model		
		R_L	q_m (mg/g)	K_L (L/mg)	R^2	K_F (mg/g)	N	R^2
Pb	95	0.0011	111	8.88	0.998	20	2.7	0.923
Cu	101	0.0009	111	11.1	0.998	16.6	2.3	0.891

Table 2: Langmuir and Freundlich isotherm constants for Pb and Cu sorption on ZnO nano particles

3.2.5. Kinetic Studies

In order to quantify kinetic data, the changes in adsorption with time, two kinetic models namely: Pseudo- first-order and pseudo-second order reactions were applied to the batch experimental data.

The pseudo first-order model is described by the following linear equation [44]:

$$\boldsymbol{Log\ (q_e - q_t) = log\ q_e - k_1 t\ /\ 2.303}$$

Where: q_e and q_t are the amount sorbed per unit mass ($mg.g^{-1}$) at equilibrium and at any time *t*, k_1 is the first order sorption rate constant (min^{-1}).The pseudo second-order model is described by the following linear equation [44]:

$$t / q_t = 1 / k_2 q_e^2 + (1/q_e) t$$

Where k_2 is the second order rate constant (g.mg^{-1} min^{-1}), q_e and q_t are the amounts of metal ion sorbed at equilibrium and at time t, respectively.

Kinetic parameters of these models are calculated from the slope and intercept of the linear plots of log (q_e- q_t) versus t and t/q_t versus t (Figure 8 and Figure 9).

Figure 8 and Figure 9 represent the relation of the pseudo-first order and second order kinetic data, respectively. From these figures K_1, q_e, K_2 and q_e are calculated and represented in Table3.

From Table3, it can be seen that the linear correlation coefficients R^2 of both Pb and Cu ions sorbed on ZnO nano particles are (0.998 and 0.999) for pseudo-first order model and (0.999 and 0.999) for pseudo-second order for both Pb and Cu respectively. Linear correlation coefficients R^2 for first and second orders are very similar especially in case of Cu. But, it is clear that the experimental adsorption capacity (q_e, experimental) and theoretical adsorption capacity (q_e, calculated) values are in better match for second order model than for first order for both Pb and Cu ions (Table3). These results suggest that the adsorption of the Pb^+ and Cu^+ ions on ZnO nano particles follows the second-order type kinetic reaction.

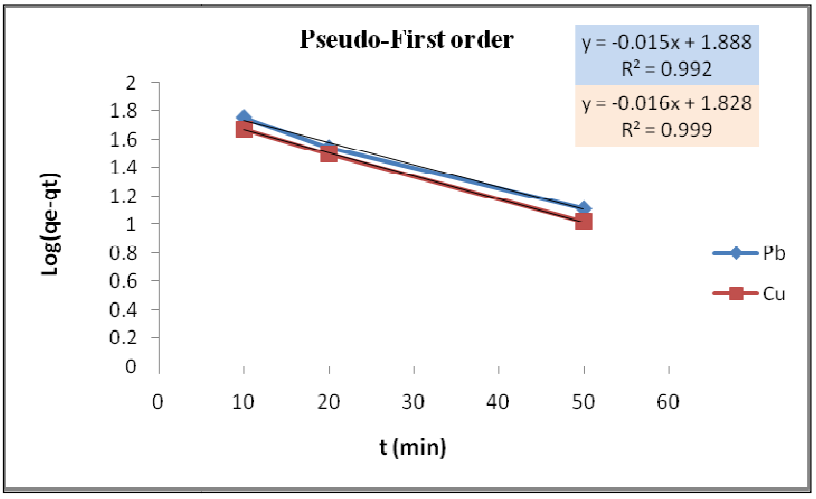

Figure 8: Pseudo-first order model for sorption of Pb(II) and Cu(II) ions onto ZnO nano particles

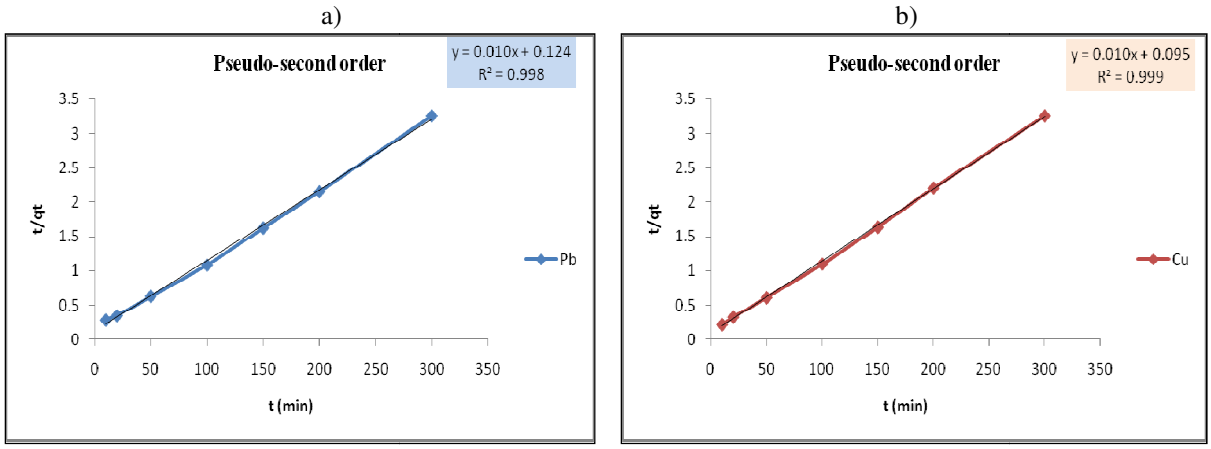

Figure 9: Pseudo-second order model for sorption of a) Pb(II) and b) Cu(II) ions onto ZnO nano particles.

Analyte Element	q_e,exp (mg/g)	Pseudo-first order			Pseudo-second order		
		K_1 (min^{-1})	q_e (mg/g)	R^2	K_2 (g/mg min)	q_e (mg/g)	R^2
Pb	92.2	0.035	77.3	0.992	0.0006	100	0.998
Cu	90.6	0.037	67.3	0.999	0.0008	100	0.999

Table 3: Kinetic parameters for the adsorption of Pb and Cu on ZnO nano particles

4. Conclusion

Different aspect ratios of hexagonal ZnO nano rods have been prepared with microwave assisted hydrothermal chemical precipitation method. The morphology of prepared nano-rods is basically dependent on the pH of the reacting solution. XRD and XRF analysis established the crystallinity and phase purity. SEM analysis has showed the rod shape of the samples. Adsorption of lead and copper

on prepared ZnO nano-rods was confirmed by ICP-OES. Adsorption parameters (pH, adsorbent dosage and contact time) were optimized. Satisfying results have been obtained. Removal percentage was increased by increasing pH value of solution until pH value 7, after that, removal percentage was kept nearly constant. The order of removal at pH 7 was Cu (97%) >Pb (92.3%). Fo ZnO dose, the optimum dosage obtained was 0.075 g/25mL (3 g/L) and the order of removal percent under this dose: Cu (93.9%)>Pb (91.7%). The optimum contact time resulted was 150 minutes and the order of removal (%) on ZnO NPs as sorbents was: Pb (92%)=Cu (92%).

5. References

i. N. Khan, T.G. Kazi, M. Tuzen, M. Soylak, Desalin. Water Treat. 55 (2015) 1088–1095.
ii. J. Han, G. Zhu, M. Hojamberdiev, J. Peng, X. Zhang, Y. Liu, B. Ge, P. Liu, New J. Chem. 39 (2015) 1874–1882.
iii. Chen YH, Li FA (2010), Colloid Inter Sci 347:277–281
iv. Ezoddina M, Shemirania F, AbdibKh, KhosraviSaghezchia M, Jamalic MR (2010), J Hazard Mater 178:900–905
v. A.Wdjtowicz, A.Stokosa, Pol.J.Environ. Stud. 11 (1) (2002) 97–101.
vi. V.C. Taty-Costodes, H.Fauduet, C.Porte, A.Delacroix, J.Hazard. Mater. B105 (2003) 121–142.
vii. A.S.AL-Hobaib, J.ElGhoul, L.ElMir, Desalination Water Treat. (2015) 1–10,
viii. M. Ulewiczi, W.Walkowliak, J.Gega,B.Pospiech, ArsSeparatoriaActa2 (2003) 47–55.
ix. K. Jainaea, K.Sanuwong, J.Nuangjamnong, N.Sukpirom, F.Unob, Chem.Eng.J. 160 (2010) 586–593.
x. Y.Feng, J.Gong, G.M.Zeng, Q.Y.Niu, H.Y.Zhang, C.G.Niu, Chem.Eng.J.162 (2010) 487–494.
xi. B.J. Pan, B.C.Pan, W.M.Zhang, L.Lv, Q.X.Zhang, S.R.Zheng, Chem.Eng. J.151 (2009) 19–29.
xii. Rahmani A, ZavvarMosavi H, Fazli M (2010),Desalination 253:94–100.
xiii. M. Ghaedi, H.Z. Khafri, A. Asfaram, A. Goudarzi, Spectrochim. Acta. Part A 152 (2016) 233–240.
xiv. Savage N, Diallo MS (2005), J Nanoparticles Res 7:331–342.
xv. Abollino O, Aceto M, Malandrino M, Sarzanini C, Mentasti E (2003), Water Res 38:1619–1627.
xvi. Sheng P, Ting YP, Chen JP, Hong L (2004), J Colloid Inter Sci 275:131–141.
xvii. Ghorbel-Abid I, Jrad A, Nahdi K, Trabelsi-Ayadi M (2009), Desalination 246:595–604.
xviii. Afkhami A, Bagheri H, Madrakian T (2011), Desalination 281:151–158.
xix. AhmadzadehTofighy M, Mohammadi T (2011), J Hazard Mater 185:140–147.
xx. Feng Y, Gong J-L, Zeng J-MNiu Q-Y, Zhang H-Y, NiuCh-G, Deng J-H, Yan M (2011), ChemEng J 162:487–494.
xxi. Navrotsky A (2000) Nanomaterials in the environment, agriculture, and technology (NEAT). J Nanoparticles Res 2:321–323.
xxii. Recillas S, Garcı´a A, Gonza´lez E, Casals E, Puntes V, Sa´nchez A, Font X (2011), Desalination 277:213–220.
xxiii. Peyghan AA, Bagheric Z (2012) Appl Surf Sci 258:8171–8176.
xxiv. Phuruangrat T, Thongtem S (2009) Mater Lett 63:1224–1226.
xxv. Hong R, Pan T, Qian J, Li H (2006) ChemEng J 119:71–81
xxvi. Liewhiran C, Seraphin S, Phanichphant S (2006) CurrAppl Phys 6:499–502
xxvii. Salavati-Niasari M, Davar F, Mazaheri M (2008) Mater Lett 62:1890–1892.
xxviii. Hua M, Zhang S, Pan B, Zhang W, Lv L, Zhang Q (2012) J Hazard Mater 211–212:317–331.
xxix. J. ElGhoul, M.Kraini, L.ElMir, J.Mater. Sci: Mater. Electron. 26 (2015) 2555–2562.
xxx. J. ElGhoul, C.Barthou, L.ElMir, Superlattices Microstruct. 51 (2012) 942–951.
xxxi. M. Hjiri, R.Dhahri, L.ElMir, A.Bonavita, N.Donato, S.G.Leonardi, G.Neri,J. Alloy. Compd. 634 (2015) 187–192.
xxxii. Fua Y, Sub Y, Lina C (2004) State Ionics 166(2004):137–146.
xxxiii. Wojciech L. Suchanek. Journal of Crystal Growth 312 (2009) 100–108.
xxxiv. X. Qiu, L. Li, J. Zheng, J. Liu, X. Sun, G. Li, J. Phys. Chem. C 112 (2008) 1242–12248.
xxxv. T. Krishna Kumar, R. Jaya Prakash, Nocola Pinna, V.N. Singh, B.R. Mehta, A.R. Phani, Mater. Lett. 63 (2009) 1063–1067.
xxxvi. ErdalSonmez, Mehmet Yilmaz, yurtcan Mustafa Tolga, Tevhit Karacali, Mehmet Ertugrul, J. Nanomater. (2012) 1–5, Article ID: 950793.
xxxvii. Amuda, O.S., Giwa, A.A., Bello, I.A., 2007. Biochemical Engineering Journal 36, p. 174.
xxxviii. Ronbanchob, A., Prasert, P., 2008. Chemical Engineering Journal 144, p. 245.
xxxix. V Venkatesham, G M Madhu, S V Satyanarayana, H.S Preetham, 2013. Procedia Engineering 51 (2013) 308 – 313.
xl. Liu Y, Cao X, Hua R, Wang Y, Liu Y, Pang C, Wang Y (2010) Hydrometallurgy 104–2:150–155
xli. Teuta S., Makfire S., Melek B., Naim H. and Avni B., **(2015)**, International journal of multidisciplinary sciences and engineering,6, 38-42.
xlii. Waly T. A., Dakroury A. M., Sayed G. E. and El-Salam S. A., **(2007)**, Eleventh International Water Technology Conference, IWTC11 Sharm El-Sheikh, Egypt.
xliii. Hamdi M. H. G., Mahmoud M. S. A. and Hisham S. H., **(2013)**, Arab Journal Of Nuclear Science And Applications, 46, 84-98.
xliv. Umit H. Kaynar, Mehmet Ayvacikli, Sermin Cam Kaynar and Umran Hicsonmez, J Radioanal Nucl Chem (2014) 299:1469–1477.